



# Three-dimensional morphologic classifications and analysis of canal isthmuses in permanent molars

Xingzhe Yin<sup>1</sup> · Jeffrey W. W. Chang<sup>2</sup> · Qianqian Wang<sup>1</sup> · Chengfei Zhang<sup>2</sup> · Xiaoyan Wang<sup>3</sup>

Received: 10 March 2021 / Accepted: 30 June 2021 / Published online: 10 July 2021  
© The Author(s), under exclusive licence to Springer-Verlag France SAS, part of Springer Nature 2021

## Abstract

**Purpose** To investigate the three-dimensional morphology of isthmuses in molars according to their boundary characteristics using micro-computed tomography (micro-CT).

**Methods** Micro-CT reconstructed images of 248 molars were evaluated. Isthmuses were classified into four types based on the boundary characteristics: isthmus with roof, isthmus with floor, band-shaped isthmus, and isthmus without boundary. The tooth and root with isthmuses, the number and location of the isthmuses in the root, and the canal configurations were recorded. The maximum of the major diameter of all canal cross-sections in one isthmus ( $d_{\max}$ ), the minor diameter of the canal in same cross-section ( $d_{\min}$ ), the distance between the  $d_{\max}$  cross-section and apex ( $D_{m-a}$ ), isthmus length ( $L_i$ ), and distance from the isthmus ending cross-section to apex ( $D_{e-a}$ ) were measured and analysed with a significance threshold set to 5%.

**Results** Isthmuses were present in 75.4% specimens. The four types of isthmuses were found in various molars and roots. Their distribution in different root locations and canal configurations was significantly different. The  $d_{\max}$ ,  $d_{\min}$ ,  $L_i$ , and  $D_{e-a}$  were analysed according to different molars and different isthmus types; their respective median values were 2.508 mm, 0.07 mm, 3.09 mm, and 3.96 mm.

**Conclusion** The three-dimensional classification of isthmuses according to the boundary characteristics provides a comprehensive picture of the isthmus in molars. Their corresponding distributions in different molars, location in roots, and canal configurations will be helpful in predicting the type of isthmus based on the tooth position and canal configurations.

**Keywords** Classification · Isthmus · Micro-computed tomography · Root canal anatomy

## Introduction

Eradication of endodontic infection by instrumentation and irrigation is considered the most important factor in the prevention and treatment of endodontic diseases [9]. However, anatomical complexities of the root canal system, such as isthmus, apical ramification, and other morphological irregularities compromise the accessibility of instruments and irrigants to effectively debride the canal of pathogenic microbes and infected/necrotic pulp tissues, which are among the major causative factors that contribute to failure of root canal therapy [11, 12].

The isthmus is a common anatomic complexity of permanent teeth [2, 3, 7], defined as a narrow, ribbon-shaped communication between two root canals that contains a fair amount of pulp tissue [19]. Most studies in the last century or in the first few years of this century were using in vitro tooth sections or transparent tooth to expose and understand

✉ Xiaoyan Wang  
wangxiaoyan@pkuss.bjmu.edu.cn

<sup>1</sup> Department of Geriatric Dentistry, Peking University School and Hospital of Stomatology, National Clinical Research Center for Oral Diseases, National Engineering Laboratory for Digital and Material Technology of Stomatology, Beijing Key Laboratory of Digital Stomatology, Beijing, China

<sup>2</sup> Endodontology, Faculty of Dentistry, The University of Hong Kong, The Prince Philip Dental Hospital, Hong Kong, China

<sup>3</sup> Department of Cariology and Endodontology, Peking University School and Hospital of Stomatology, National Clinical Research Center for Oral Diseases, National Engineering Laboratory for Digital and Material Technology of Stomatology, Beijing Key Laboratory of Digital Stomatology, No.22, Zhongguancun South Avenue, Haidian District, Beijing 100081, China

isthmus morphology. Thus, the classic isthmus classifications, such as Weller's and Hsu and Kim's, are all based on the configuration of root sections [4, 19]. These classifications were widely used in many research studies, including those using micro-CT [8, 10], and they have more practical clinical value for apical root surgery [18]. However, the two-dimensional classifications cannot fully reflect the actual three-dimensional morphologic features of the isthmuses. Fan et al. first proposed a three-dimensional classification of isthmus in 2010 [3]. However, their study only observed the apical 5-mm canal system of the mesial root of mandibular molars. Since isthmus exists in the apical portion as well as the middle and cervical portions of the root canal system, it is important to evaluate the morphology of the isthmus within the entire root canal system instead of focussing only on the apical 5-mm canal.

Thus, on the basis of previous studies, we attempted to investigate the morphology of the isthmus in human maxillary and mandibular molars, classified isthmuses according to the three-dimensional morphology and analysed some measurements of the isthmus quantitatively and qualitatively using micro-CT. We believe these findings may provide a comprehensive picture of the isthmus in molars, and useful data for further study.

## Materials and methods

### Specimen selection

The present study was approved by the Ethics Committee of the Peking University School of Stomatology (No. PKUS-SIRB-201840196). The molar teeth were collected from a pool of teeth that were extracted because of periodontal disease. All teeth were intact with fully formed apices, no restorations, cracks, fractures, or endodontic treatment. Teeth that had a C-shaped canal as seen in micro-CT images were excluded. A total of 103 maxillary molars and 145 mandibular molars were included in this study.

### Micro-CT scanning and three-dimensional reconstruction

The teeth were mounted in a 7-mm-diameter plastic container on the scanning platform with the root oriented vertically and then scanned using a micro-CT scanner (Sky-Scan 1172 Desktop X-ray microtomograph, Aartselaar, Belgium) at an isotropic resolution of 26.73  $\mu\text{m}$ . The X-ray tube was operated at 80 kV/100  $\mu\text{A}$ . Transmission X-ray images were recorded at two rotational steps for 360° rotation. Images of each specimen were reconstructed using dedicated software (NRecon v. 1.6.9.18 Bruker-microCT), providing axial cross-section images. Three-dimensional reconstruction models were rendered for inspection of the canal systems using CTAn software (v1.10.1.0, Bruker-microCT) and CTVol software (v2.1.1.2, Bruker-microCT). To enhance the visualisation of the fine root canal structure, segmented volumes of the canal structure were represented by an opaque red colour, and the external morphology of the root was rendered as grey translucency.

### Classifications and measurements of the isthmuses

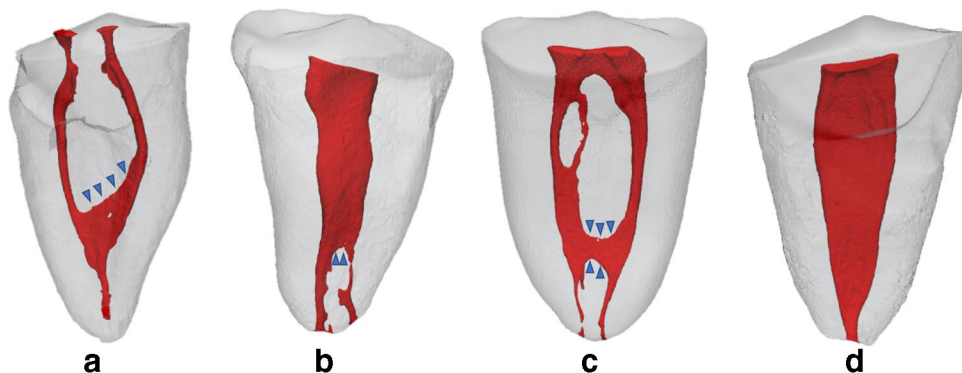
Three-dimensional reconstructions of root canal morphology were observed from different angles using CTVol Software (v2.1.1.2, Bruker-microCT). According to the boundary characteristics, each isthmus was assigned to one of four categories (Fig. 1):

Type I, isthmus with a roof: isthmus between two canals with a coronal boundary only; the rest was connected with the main root canal or open to the apex.

Type II, isthmus with a floor: isthmus between two canals with an apical boundary only; the rest was connected with the main root canal or open to the pulp chamber.

Type III, band-shaped isthmus: isthmus between the two canals with both coronal and apical boundaries; it appeared like a band connected to the two canals.

**Fig. 1** Classification of isthmuses. **a** Type I, isthmus with a roof; **b** Type II, isthmus with a floor; **c** Type III, band-shaped isthmus; **d** Type IV, isthmus without boundaries. The blue arrow indicates the boundary of the isthmus



Type IV, isthmus without a boundary: a complete connection between the two canals from the pulp chamber to the apex.

The teeth and roots with isthmus, the number and position of isthmus in the root, and root canal configuration were recorded. Each isthmus was observed cross-sectionally using CTAn software (v1.10.1.0, Bruker-microCT), and the following measurements were taken (Fig. 2):  $d_{\max}$  was taken as the maximum of the major diameter of all canal cross-sections in one isthmus; then in the same cross-section, the minor diameter of the canal was recorded as  $d_{\min}$ ; and the distance from this cross-section to the anatomical apex was recorded as  $D_{m-a}$ ;  $L_i$  was the axially continuing length of the isthmus, which was the length from the cementoenamel junction (CEJ) or isthmus roof to isthmus floor or isthmus ending cross-section; and  $D_{e-a}$  was the distance from the isthmus floor or isthmus ending cross-section to the anatomical apex. The isthmus roof was located by the cross-section where the two canals merged, and the isthmus floor was located by the cross-section where the two canals redivided, as described by Keleş and Keskin [5]. For isthmuses without apical boundary (such as Type I and IV), the isthmus ending cross-section was located when the ratio of major diameter to minor diameter of the canal cross-section was less than 2, which the two root canals converge in one at that level. And based on the measured position ( $D_{m-a}$ ) of cross-section of  $d_{\max}$  in root, the data of the  $d_{\max}$  and  $d_{\min}$  were divided into three groups, which were apical portion ( $D_{m-a} \leq 4$  mm), middle portion ( $4 \text{ mm} < D_{m-a} \leq 8$  mm) and cervical portion ( $D_{m-a} > 8$  mm), for analysis.

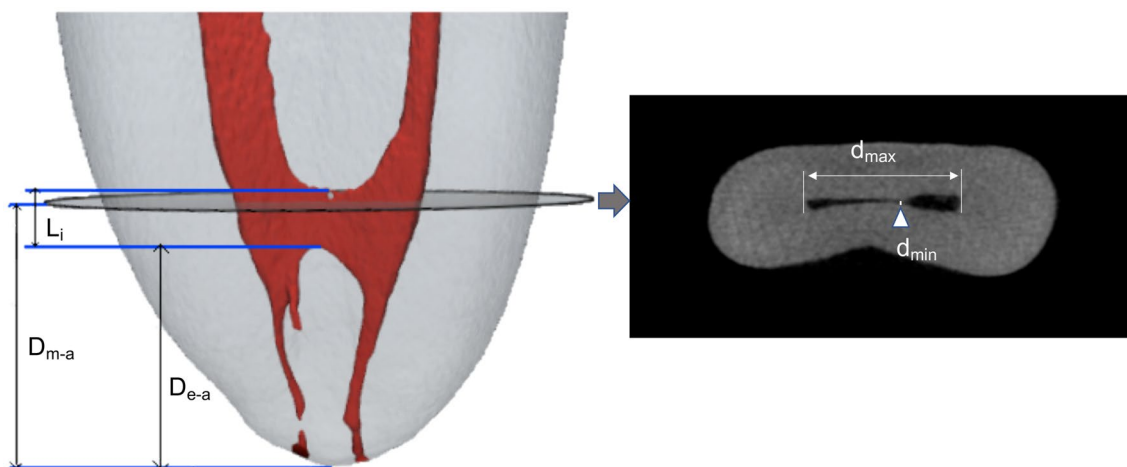


**Fig. 2** The measurement method of the measured value of the isthmus.  $d_{\max}$ : the maximum of the major diameter of all canal cross-sections in one isthmus;  $d_{\min}$ : the minor diameter of the canal in the same cross-section;  $D_{m-a}$ : the distance from the cross-section, which

## Statistical analysis

Statistical analysis was performed using SPSS software (v.24, IBM Corporation, Armonk, NY, USA). Differences in the distribution of types of isthmuses according to tooth position, location in the root, and canal configuration were compared using chi-square test. Nonparametric tests were used to analyse the difference in value of measurements of the isthmuses except the data of  $d_{\max}$  according to isthmus classifications. General linear model univariate analysis and one-way ANOVA test were used due to the data of  $d_{\max}$  are normally distributed. Differences were considered statistically significant when  $P < 0.05$ .

## Results

### The incidence, distribution and measurements of isthmuses according to tooth position

In all, 253 isthmuses were found in 187 teeth, accounting for 75.4% of all specimens. Overall, 216 roots were identified with isthmuses; 182 (84.3%) had one isthmus, 31 (14.4%) had two isthmuses, and 3 (1.4%) had three isthmuses.

The incidence and distribution of isthmuses in molars are shown in Table 1. In maxillary molars, Type II and III isthmuses were observed more frequently, whereas mandibular molars had more Type I and IV isthmuses. There was a significant difference in the isthmus types among tooth positions (Pearson's chi-square test,  $P = 0.003$ ).

The measurements of isthmus in different molars are presented in Table 2. The measured values of  $d_{\max}$  and  $L_i$  in mandibular molars were greater than those in maxillary

the  $d_{\max}$  and  $d_{\min}$  were taken from, to the anatomical apex;  $L_i$ : the axially continuing length of the isthmus;  $D_{e-a}$ : the distance from the isthmus floor or isthmus ending cross-section to the anatomical apex

**Table 1** Incidence and distribution of isthmuses in molars

Tooth	N	N(t) (%)	N(i)	Types of isthmus n (%) <sup>a</sup>			
				Type I	Type II	Type III	Type IV
Maxillary first molar	42	27 (64.3)	34	7 (20.6)	7 (20.6)	13 (38.2)	7 (20.6)
Maxillary second molar	61	33 (54.1)	38	2 (5.3)	19 (50.0)	10 (26.3)	7 (18.4)
Mandibular first molar	67	57 (85.1)	90	24 (26.7)	23 (25.6)	16 (17.8)	27 (30.0)
Mandibular second molar	78	70 (89.7)	91	21 (23.1)	28 (30.8)	11 (12.1)	31 (34.1)

N number of samples; N(t) number of teeth with isthmuses, the percentages showed the incidence of isthmuses; N(i) number of isthmuses

<sup>a</sup>Pearson's chi-square test:  $P=0.003$

**Table 2** Median values for  $d_{\max}$ ,  $d_{\min}$ ,  $L_i$  and  $D_{e-a}$  in molars

Tooth	N	$d_{\max}$ (mm) <sup>a</sup>	$d_{\min}$ (mm) <sup>b</sup>	$L_i$ (mm) <sup>a</sup>	$D_{e-a}$ (mm) <sup>b</sup>
		Median (Q1, Q3)	Median (Q1, Q3)	Median (Q1, Q3)	Median (Q1, Q3)
Maxillary first molar	34	2.014 (1.601, 2.421)	0.069 (0.047, 0.114)	1.994 (0.997, 4.424)	3.944 (2.175, 5.651)
Maxillary second molar	38	1.731 (1.422, 2.352)	0.073 (0.053, 0.138)	1.966 (1.343, 4.251)	4.024 (2.099, 5.561)
Mandibular first molar	90	2.697 (2.224, 3.131)	0.073 (0.050, 0.153)	3.472 (1.858, 6.156)	3.596 (1.898, 5.388)
Mandibular second molar	91	2.725 (2.181, 3.204)	0.070 (0.050, 0.113)	3.075 (1.310, 5.668)	3.583 (2.139, 6.176)

N number of isthmuses;  $d_{\max}/d_{\min}$  the major and minor diameters of the canal in the isthmus;  $L_i$  the length of the isthmus;  $D_{e-a}$  the distance from the isthmus floor or isthmus ending cross-section to the anatomical apex; Q1 first quartile; Q3 third quartile

<sup>a</sup>Kruskal–Wallis test  $P < 0.05$

<sup>b</sup>Kruskal–Wallis test  $P > 0.05$

molars, and the differences were statistically significant (Kruskal–Wallis test,  $P < 0.05$ ). There was no significant difference in  $d_{\min}$  and  $D_{e-a}$  according to different tooth positions (Kruskal–Wallis test,  $P > 0.05$ ).

### The distribution and measurements of isthmuses according to isthmus classifications

Different types of isthmuses were present in different locations of roots or in different canal configurations (Pearson's chi-squared test,  $P < 0.001$ ). Type I isthmuses appeared more in the apical region and were all found in the root with merged or intersected canals, while Type II isthmuses occurred more in the cervical third of the root with canals divided from one. The detailed distribution is shown in Fig. 3.

The  $d_{\max}$  and  $d_{\min}$  of different types of isthmuses were marked and analysed in three groups (Fig. 4a, b). The mean of  $d_{\max}$  were significantly different when in different root portion group (General Linear Model Univariate Analysis and Bonferroni's test,  $P < 0.001$ ), but there was no difference in isthmus types within same group (one-way ANOVA,  $P > 0.05$ ). For  $d_{\min}$ , there was no statistically difference among root portion groups (Scheirer-Ray-Hare test,  $P = 0.456$ ), while there were significant differences between some isthmus types in middle portion and cervical portion group (Kruskal–Wallis test,  $P < 0.001$ ).

The median  $L_i$  for Types I–IV were 2.11 mm, 2.09 mm, 1.54 mm, and 6.22 mm, respectively. There was a significant difference between Type IV and other types (Kruskal–Wallis test,  $P < 0.001$ ) (Fig. 4c).

Of the 253 isthmuses, the  $D_{e-a}$  of 104 (41.1%) isthmuses was within 3 mm. Additionally, the median  $D_{e-a}$  for Types I–IV were 2.49 mm, 7.06 mm, 3.49 mm, and 3.60 mm, respectively (Fig. 4d).

## Discussion

Successful root canal therapy requires thorough knowledge of the root canal anatomy and conceivable anatomical variations. Isthmuses are some of the most common but complicated anatomical variations in the root canal system, presenting a formidable challenge for root canal shaping, cleaning, and obturation [1, 16]. It has been reported that any tooth root with more than one root canal is likely to contain an isthmus [14]. In this study, the incidence of isthmus was 64.3%, 54.1%, 85.1%, and 89.7% in the maxillary first molars, maxillary second molars, mandibular first molars, and mandibular second molars, respectively. These results are similar to those of previous studies on maxillary and mandibular first molars [2, 3, 13, 15, 18, 21], and slightly higher than those reported on maxillary and mandibular second molars [2, 3, 7, 20]. These differences may be because

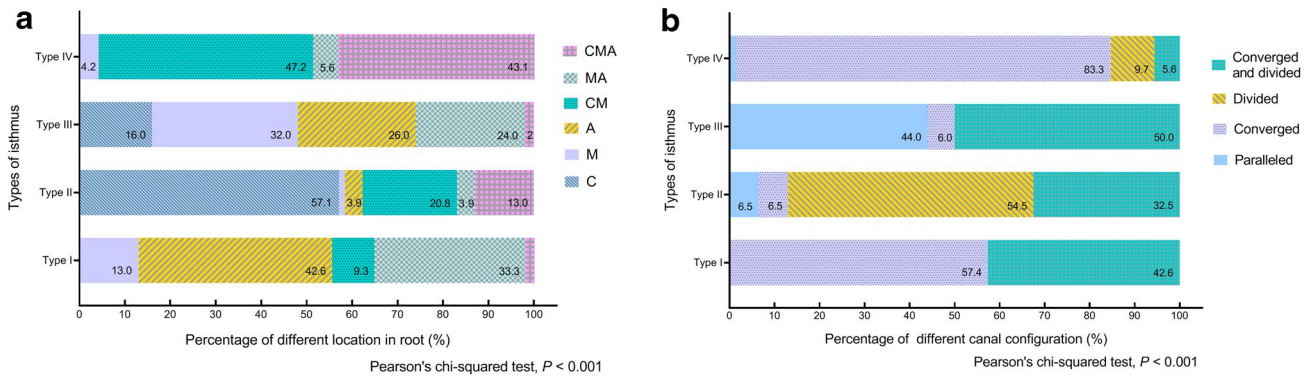


**Fig. 3** Distribution of the types of isthmuses in different canal locations or canal configurations. **a** C: the cervical third of the root canal; M: the middle third of the root canal; A: the apical third of the root canal; CM: from the cervical third to the middle third of the root canal; MA: from the middle third to the apical third of the root canal;

**b** Paralleled: the canals are basically parallel from the orifice to the apex; converged: the canals are converged together; Divided: the canals are divided into two or more canals; converged and divided: the canals both have converged and divided parts

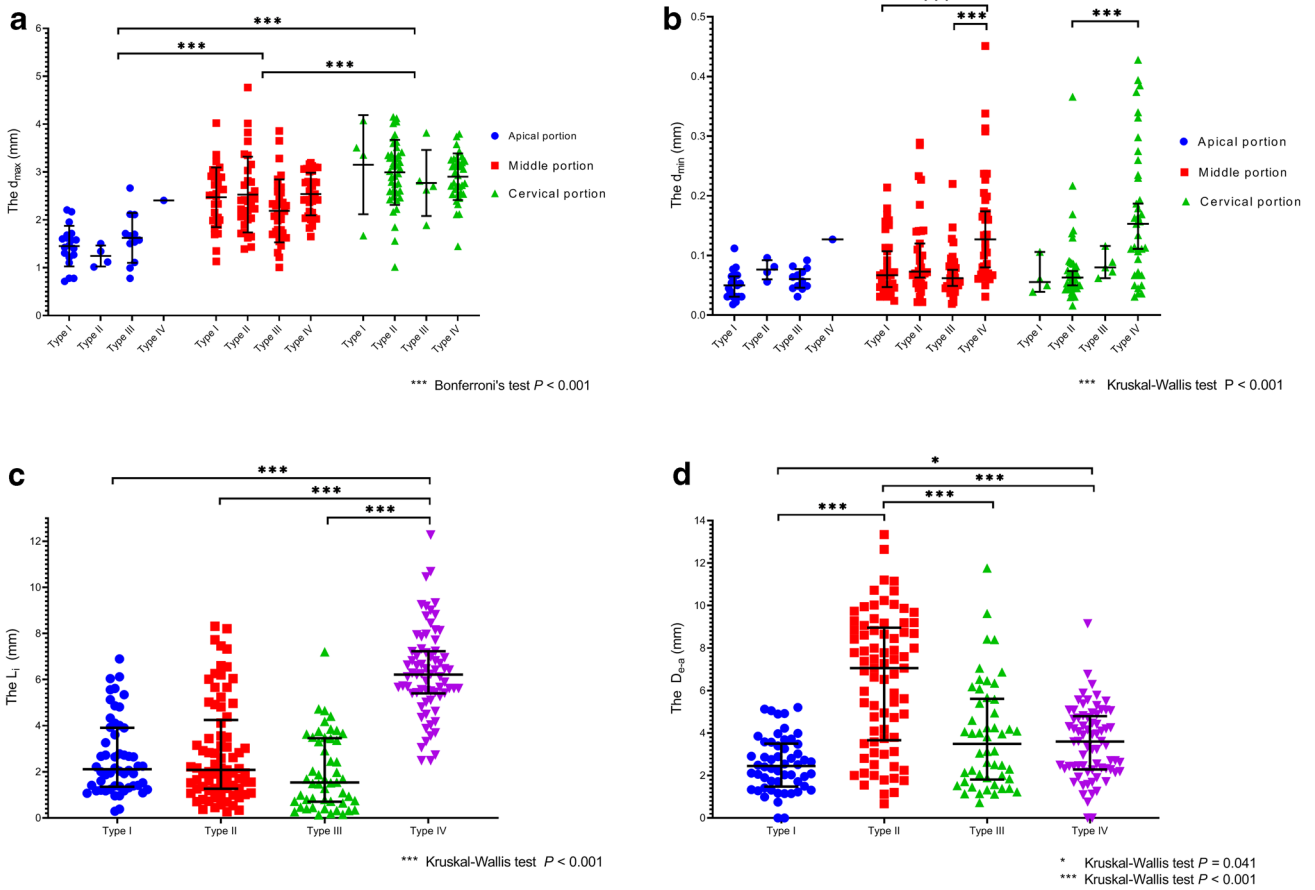


**Fig. 4** The measurements of isthmuses. **a** The black lines represent the mean and standard deviations. **b–d** The black lines represent the medians and interquartile ranges

of the smaller number of samples and the different methods used in previous studies on maxillary and mandibular second molars.

Terms like ‘isthmus roof’, ‘isthmus floor’, and ‘band-shaped isthmus’ have been used to describe isthmic boundaries or morphology in previous studies [5, 6]. On this basis, after observing and comparing 253 three-dimensional reconstructed isthmus configurations, four types of isthmus were classified according to the boundary characteristics in this study. Different from the previous classifications, which were focussed on the morphological description of the root canal section or local intercanal connection, grasping the characteristics of the number and location of the isthmus boundary can not only get rid of the dilemma of describing the ever-changing isthmus morphology but also show some relationship between the isthmus type and canal configuration.

The Vertucci classification is widely used to record canal configuration [17]. In the present study, the canal configurations were recorded as paralleled, converged, divided, and converged and divided. The paralleled canal could also be described as Vertucci type IV or VIII; converged canal, as Vertucci type I or II; divided canal, as Vertucci type V; and converged and divided as Vertucci type III, VI, or VII. According to the results shown in Fig. 3b, Type I isthmuses were all found in canal configurations of Vertucci types II, III, VI, or VII. Further, 87.0% Type II isthmuses were found in Vertucci types V or VII; Type III isthmuses most likely appeared in Vertucci type IV, VI, and VIII; and most Type IV isthmuses were of Vertucci type I. Sample size and heterogeneity limit the in-depth exploration of the relationship between the isthmus type and the canal configuration in this study. However, these results may still help dentists estimate the occurrence and type of isthmus, when the canal configuration is identified clinically through preoperative radiography or intraoperative exploration.

Three- and two-dimensional measurements have been taken to reveal the complex shapes of the isthmuses in previous studies [3, 5]. The measurements in the present study also show some characteristics. Such as, the  $d_{max}$  of the cervical portion of the root was significantly larger than that in the apical portion, which was consistent with the root shape narrowing apically, but the difference in  $d_{min}$  was more related to isthmus type than the portion of the root, and Type IV isthmuses were significantly wider and longer than those in other types. However, it's important to emphasize that, the value of  $d_{max}$  and  $d_{min}$  were taken in the same cross-section in the present study, as it is almost impossible to visually identify the most minor diameter of the canal of all layers in one isthmus. And the measurement values were also affected by many other factors, such as the angle of the tooth placement during the scan, the curvature of the root, the setting of the threshold during the three-dimensional reconstruction, the human error of the

selected point during the measurement, and so on. Therefore, all measurement values are recommended as a reference to assist dentists in understanding the order of magnitude of isthmus size and characteristics of each type of isthmus.

## Conclusions

The three-dimensional classification of isthmuses according to the boundary characteristics provide a new perspective and a comprehensive picture of the isthmus in molars. Their corresponding distributions in different teeth, location in roots, and canal configurations will be helpful in predicting the type of isthmus based on the tooth position and canal configurations.

**Supplementary Information** The online version contains supplementary material available at <https://doi.org/10.1007/s00276-021-02796-5>.

**Acknowledgements** The authors are sincerely thankful for Prof. Bin Fan's insightful opinions, from the Hospital of Stomatology, Wuhan University. This work was supported by the National Key Research and Development Programme of China (2017YFC1104300/4303/4301).

**Author contribution** XZ Yin: Data collection, Data management, Data analysis, Manuscript writing and revising. J WW Chang: Project development, Data collection, Manuscript revising. QQ Wang: Data collection, Data analysis. CF Zhang: Project development, Manuscript revising. XY Wang: Project development, Manuscript revising.

**Funding** This work was supported by the National Key Research and Development Programme of China (2017YFC1104300/4303/4301).

**Availability of data and material** Data are available on demand.

**Code availability** Not applicable.

## Declarations

**Conflict of interest** The authors deny any conflicts of interest related to this study.

**Ethical approval** All procedures performed in studies involving human participants were in accordance with the ethical standards of the institutional and national research committee and with the 1964 Helsinki Declaration and its later amendments or comparable ethical standards. The study was approved by the Ethics Committee of the Peking University School of Stomatology (No. PKUSSIRB-201840196).

**Consent to participate** Not applicable.

**Consent for publication** Not applicable.

## References

1. De-Deus G, Marins J, Neves Ade A, Reis C, Fidel S, Versiani MA, Alves H, Lopes RT, Paciornik S (2014) Assessing accumulated hard-tissue debris using micro-computed tomography and free

- software for image processing and analysis. *J Endod* 40:271–276. <https://doi.org/10.1016/j.joen.2013.07.025>
2. Estrela C, Rabelo LE, de Souza JB, Alencar AH, Estrela CR, Sousa Neto MD, Pecora JD (2015) Frequency of root canal isthmi in human permanent teeth determined by cone-beam computed tomography. *J Endod* 41:1535–1539. <https://doi.org/10.1016/j.joen.2015.05.016>
  3. Fan B, Pan Y, Gao Y, Fang F, Wu Q, Gutmann JL (2010) Three-dimensional morphologic analysis of isthmuses in the mesial roots of mandibular molars. *J Endod* 36:1866–1869. <https://doi.org/10.1016/j.joen.2010.08.030>
  4. Hsu YY, Kim S (1997) The resected root surface. The issue of canal isthmuses. *Dent Clin N Am* 41:529–540
  5. Keleş A, Keskin C (2018) A micro-computed tomographic study of band-shaped root canal isthmuses, having their floor in the apical third of mesial roots of mandibular first molars. *Int Endod J* 51:240–246. <https://doi.org/10.1111/iej.12842>
  6. Keleş A, Keskin C (2017) Apical root canal morphology of mesial roots of mandibular first molar teeth with vertucci Type II configuration by means of micro-computed tomography. *J Endod* 43:481–485. <https://doi.org/10.1016/j.joen.2016.10.045>
  7. Lima FJ, Montagner F, Jacinto RC, Ambrosano GM, Gomes BP (2014) An in vitro assessment of type, position and incidence of isthmus in human permanent molars. *J Appl Oral Sci* 22:274–281. <https://doi.org/10.1590/1678-775720130585>
  8. Marceliano-Alves MF, Lima CO, Bastos L, Bruno AMV, Vidaurre F, Coutinho TM, Fidel SR, Lopes RT (2018) Mandibular mesial root canal morphology using micro-computed tomography in a Brazilian population. *Aust Endod J* 45:51–56. <https://doi.org/10.1111/aej.12265>
  9. Markus Haapasalo UE, Zandi H, Coli JM (2005) Eradication of endodontic infection by instrumentation and irrigation solutions. *Endod Top* 10:77–102. <https://doi.org/10.1111/j.1601-1546.2005.00135.x>
  10. Mehrvarzfar P, Akhlagi NM, Khodaei F, Shojae G, Shirazi S (2014) Evaluation of isthmus prevalence, location, and types in mesial roots of mandibular molars in the Iranian Population. *Dent Res J (Isfahan)* 11:251–256
  11. Nair PN, Henry S, Cano V, Vera J (2005) Microbial status of apical root canal system of human mandibular first molars with primary apical periodontitis after “one-visit” endodontic treatment. *Oral Surg Oral Med Oral Pathol Oral Radiol Endod* 99:231–252. <https://doi.org/10.1016/j.tripleo.2004.10.005>
  12. Siqueira JF, Alves FRF, Versiani MA, Rôças IN, Almeida BM, Neves MAS, Sousa-Neto MD (2013) Correlative bacteriologic and micro-computed tomographic analysis of mandibular molar mesial canals prepared by self-adjusting file, reciproc, and twisted file systems. *J Endod* 39:1044–1050. <https://doi.org/10.1016/j.joen.2013.04.034>
  13. Tam A, Yu DC (2002) Location of canal isthmus and accessory canals in the mesiobuccal root of maxillary first permanent molars. *J Can Dent Assoc* 68:28–33
  14. Teixeira FB, Sano CL, Gomes BP, Zaia AA, Ferraz CC, Souza-Filho FJ (2003) A preliminary in vitro study of the incidence and position of the root canal isthmus in maxillary and mandibular first molars. *Int Endod J* 36:276–280. <https://doi.org/10.1046/j.1365-2591.2003.00638.x>
  15. Verma P, Love RM (2011) A Micro CT study of the mesiobuccal root canal morphology of the maxillary first molar tooth. *Int Endod J* 44:210–217. <https://doi.org/10.1111/j.1365-2591.2010.01800.x>
  16. Verstraeten J, Jacquet W, De Moor RJG, Meire MA (2017) Hard tissue debris removal from the mesial root canal system of mandibular molars with ultrasonically and laser-activated irrigation: a micro-computed tomography study. *Lasers Med Sci* 32:1965–1970. <https://doi.org/10.1007/s10103-017-2297-4>
  17. Vertucci FJ (1984) Root canal anatomy of the human permanent teeth. *Oral Surg Oral Med Oral Pathol Oral Radiol Endod*. [https://doi.org/10.1016/0030-4220\(84\)90085-9](https://doi.org/10.1016/0030-4220(84)90085-9)
  18. von Arx T (2005) Frequency and type of canal isthmuses in first molars detected by endoscopic inspection during periradicular surgery. *Int Endod J* 38:160–168. <https://doi.org/10.1111/j.1365-2591.2004.00915.x>
  19. Weller RN, Niemczyk SP, Kim S (1995) Incidence and position of the canal isthmus. Part 1. Mesiobuccal root of the maxillary first molar. *J Endod* 21:380–383. [https://doi.org/10.1016/s0099-2399\(06\)80975-1](https://doi.org/10.1016/s0099-2399(06)80975-1)
  20. Wolf TG, Paque F, Woop AC, Willershausen B, Briseno-Marroquin B (2017) Root canal morphology and configuration of 123 maxillary second molars by means of micro-CT. *Int J Oral Sci* 9:33–37. <https://doi.org/10.1038/ijos.2016.53>
  21. Yu DC, Tam A, Chen MH (1998) The significance of locating and filling the canal isthmus in multiple root canal systems. A scanning electron microscopy study of the mesiobuccal root of maxillary first permanent molars. *Micron* 29:261–265. [https://doi.org/10.1016/s0968-4328\(98\)00063-8](https://doi.org/10.1016/s0968-4328(98)00063-8)

**Publisher's Note** Springer Nature remains neutral with regard to jurisdictional claims in published maps and institutional affiliations.